

Simulation and verification of Thomson actuator systems

A. Bissal, E. Salinas, G. Engdahl, and M. Ohrstrom

Abstract—The inherent characteristics of Thomson coil's (TC) are appropriate to meet the needs of high speed actuators for mechanical switching devices in so-called smart grids. This is due to the large forces that it can exert in the time scale of milliseconds. A coupled COMSOL Multiphysics model is developed in 2D involving PSpice circuits, Magneto-statics, and Moving Mesh Mode for predicting the motion of a conductive armature in the proximity of a coil upon an impulsive discharge of a capacitor bank. In the present work, the forces and the acceleration of an aluminum ring are computed. Subsequently, different case studies are explored to better understand the variables involved and their degree of influence they have on the TC. The developed model was validated experimentally with a built prototype and the results show that it can be used to accurately predict the performance of high speed actuators.

Index Terms— high speed actuators, smart grids, Magneto-statics, moving mesh

I. INTRODUCTION

Understanding the behavior of a Thomson coil (TC) has many advantages because it is related to numerous applications, from robotics, levitation and transport to high voltage power systems. In fact, due to its properties as a fast actuator, several studies have been conducted on TCs and their applications in high speed protection systems and hybrid circuit breakers [2,5,6,7,11,12,13,14,15].

The TC was named after Elihu Thomson. Later on, Noel Barry discovered how to levitate a conducting non-magnetic round ring above a helix shaped Thomson coil excited by an AC source. He also devised a control strategy to modulate the amplitude of the AC source in such a way that the ring stays in a stationary levitated position [1].

The need for high speed circuit breakers is rising and TCs are often constructed without proper modeling, design, and optimization. In this paper, a simulation of a working model of a Thomson coil is carried out using COMSOL to thoroughly study the physics behind it. However, simulations alone are not enough to validate the results. Accordingly, to add credibility, the model is validated by experimental verification. After validation, the behavior of the flux lines and their contribution to the exerted force on the aluminum disk are studied paving a way for future optimization.

II. MODELING

The TC shown in Figure 1 is implemented in COMSOL version 3.5a. A Multiphysics model is used based on magneto statics, moving mesh mode (ale), and PSPICE circuits to

model the electric circuitry. The TC is chosen to be modeled in the rz-plane where the horizontal axis represents the r-axis and the vertical axis represents the z axis. The TC can be approximated by a 2D axial-symmetric model where the coil turns will be represented as rectangles of the same dimension as their cross sections (2 x 4 mm). To represent the enameled coating, an inter distance separation of 0.1mm will be taken into account between the coil turns. As for the aluminum disk, it will be represented as a rectangle with a width equal to the difference between the outer and inner radii and a height equal to its thickness. Moreover, the geometry is unchanged when rotated about the vertical axis passing through the center of the coil. As a result, one can make use of this axial symmetry to define half the geometry. Figure 2 shows a sketch of the 2D axial symmetric representation of the TC. The Aluminum is in grey color, the coil turns are in orange, the surrounding air in white, and the symmetry line is represented as a dashed black line.

The electrical representation is shown in Figure 3. The TC is powered by a 33 mF capacitor bank. A diode is connected in parallel to the capacitor to protect it from negative voltage. The capacitor bank series resistance and the total inductance of the connecting wires and belonging loop circuit are represented by R_{stray} and L_{stray} .

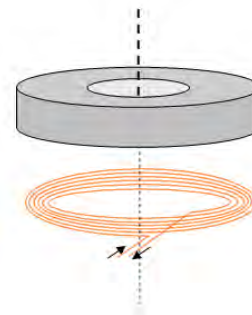


Figure 1 TC schematic

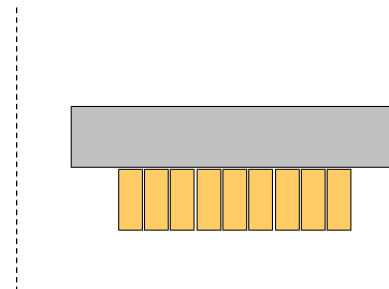


Figure 2 2D axial-symmetric representation of the TC

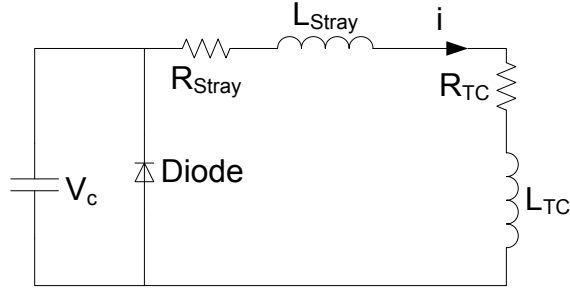


Figure 3 Electric circuit

III. AN ANALYTICAL FORCE ESTIMATION FOR THE ORIGINAL TC RING TOPOLOGY

Maxwell's equations serve as the key point to understand the theory behind the TC. When an alternating voltage source is connected across the terminals of a coil, a sinusoidal current $i_c = I_c \sin(\omega t)$ will flow through it [4,8,9]. This current will produce a magnetic field. The flux density directed along the normal axis of the coil is:

$$B(t) = B_c(r, z) \sin(\omega t) \quad (1)$$

, where \hat{B}_c is the peak amplitude of the flux density. Not all flux through the coil will go through the aluminum ring of radius b since some flux lines will exit in between the coil and the aluminum ring. The flux can be represented by two components, a radial flux density $B_r = B_r \sin(\omega t)$ and a vertical flux density $B_z = B_z \sin(\omega t)$. According to Lenz's law, since there is a time variable magnetic flux, currents will be induced in the aluminum ring. Thus, as the magnetic flux increases, currents are induced in the aluminum disk producing their own magnetic field in the opposite direction to decrease the offset. Applying Faradays's law [3]:

$$\nabla \times \mathbf{E} = - \frac{\partial \mathbf{B}}{\partial t} \quad (2)$$

the electric field intensity is given as [1]:

$$E(r, t) = - \frac{\omega r \hat{B}_z}{2} \cos(\omega t) \quad (3)$$

The electric field strength is directed along the circumference of the aluminum ring. The induced voltage in the aluminum ring is:

$$v_{Al} = \oint_l E \cdot dl = - \frac{\omega 2\pi r^2 \hat{B}_z}{2} \cos(\omega t) \quad (4)$$

A current in the ϕ direction is produced as a result of the z component of the field:

$$i_\phi = \frac{v_{Al}}{Z_{Al}} \quad (5)$$

Z_{Al} is the impedance of the aluminum ring.

The current in the ϕ direction and the radial component of the field result in a vertically directed force given by:

$$F_z = \pi b I_\phi B_r \sin \phi_r \quad (6)$$

, where I_ϕ is the amplitude of the ring current and ϕ_r the ring phase shift.

To sum up, the force exerted on the ring is proportional to the induced current in the phi direction multiplied by the radial component of the magnetic flux density. The greater the magnetic flux density, the greater the force and acceleration. To simulate the displacement x of the aluminum disk versus time, one has to include Newton's second law,

$$F_{Total} = ma \quad (7)$$

Where,

$$a = \ddot{x} \quad (8)$$

IV. EXPERIMENTAL VERIFICATION

A custom prototype is built that consists of a 9 turn copper coil embedded in epoxy. The coil is glued to the inside of a Bakelite frame. Bakelite is used because it is non-conductive and as a result, no eddy currents will be induced in it. The bottom steel plate is clamped to the table to prevent any movement. The top plate is also made of Bakelite with a thin layer of rubber to damp the motion of the aluminum ring. A high speed camera is used to record the movement of the aluminum ring. The camera is triggered by an oscilloscope that sends a trig signal as soon as the capacitor bank starts to discharge. Three series of tests were carried out.

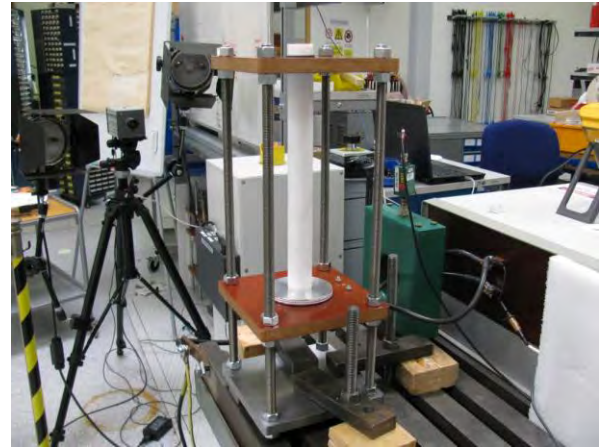


Figure 4 Custom built prototype

The aim of the first test setup is to be able to approximate the stray impedance without any influence from the aluminum ring. First, a 33 mF capacitor bank is discharged in the coil with no aluminum ring on top at three voltage levels 25, 50, and 100V to record the current pulses. Second, the coil impedance has to be measured. However, the frequency at which to measure the coil impedance is hard to determine. Consequently, the resistance and inductance of the coil are

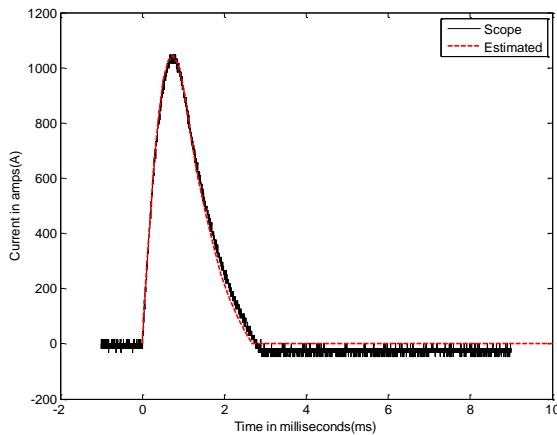
determined by discharging the 33 mF capacitor bank in a COMSOL simulation with no aluminum disk in proximity. The resistance is deduced by integrating the ohmic power losses over the 9 coil sub domains and diving by the square of the current. As for the inductance, it is calculated from the magnetic energy which is given by:

$$L = \frac{2\omega_m}{i^2} \quad (9)$$

At low values of current, the impedance is neglected. The resistance showed to be 4.62 mΩ and the inductance is 7.44 μH respectively. Finally, the only unknown was the stray impedance. It was estimated by fitting the measured current pulses from the lab with the obtained current pulses from the following differential equations in MATLAB:

$$\begin{aligned} \frac{dV_C}{dt} &= -\frac{i}{C} \\ \frac{di}{dt} &= \frac{1}{L + L_{Stray}}(V_C - R_{Stray}i - R_{TC}i) \end{aligned} \quad (10)$$

The curve fits for the current from the oscilloscope and the solution of the differential equations for a stray resistance of 4 mΩ and an inductance of 1.5 μH as shown in Figure 5, Figure 6, and Figure 7. The current pulses at the different voltage levels for the chosen stray impedance fit with high ac



Fi

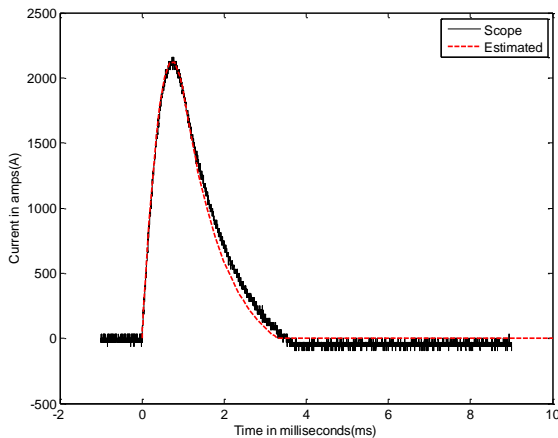


Figure 6 Current pulse at 50 V

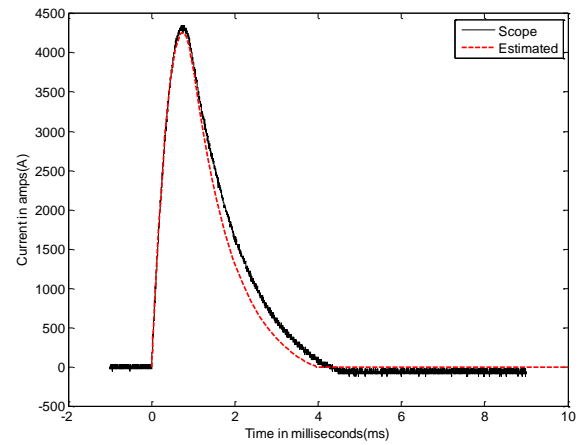


Figure 7 Current pulse at 100 V

In the second test, the capacitor bank was discharged at with a Teflon cylinder to guide the aluminum ring. Teflon is used because the material is nonconductive and has small friction.

In the third test, the Teflon guide was removed but the TC was caged in Plexiglas to account for safety. The guide was omitted to eliminate friction and observe the trajectory of the aluminum ring. Tests, 2 and 3 showed identical results verifying that the TC shoots the aluminum ring vertically upwards without touching the Teflon guide. Figure 8 shows the aluminum ring displacement versus time as well as the displacement signal from the high speed camera for several tests at 50 V excitation level. The COMSOL simulation fits with the measured data with good accuracy. The discrepancy is due to the following reasons:

- The coil is modeled as concentric rings in COMSOL and not as a spiral
- Air resistance is neglected
- The impedance of the coil is not 100% accurate
- The stray impedance is not constant
- The discharged voltage from the capacitor bank is not

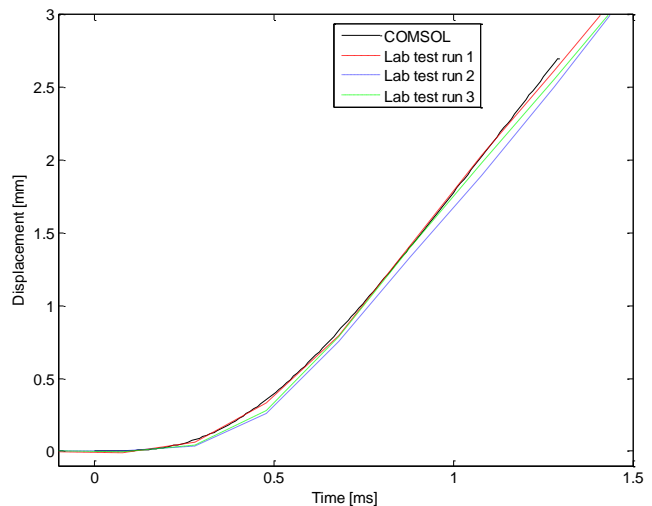


Figure 8 COMSOL simulation in comparison to measured lab data

V. RESULTS

In figures 9-12 results from a simulation are shown when a 7 mF capacitor bank initially charged to 400 V is discharged through the TC producing an impulsive current of the order of ten thousand amperes. The stray resistance of the wires is approximately 10 mΩ and the stray inductance is 1μH. The capacitor voltage starts at 400 V and then decays exponentially, see Figure 9. Due to this applied voltage, the current rises and reaches a peak value of 10 kA in 0.2 milliseconds as shown in Figure 10. This results in circulating time-varying magnetic field lines. The direction and amplitude of the magnetic field are shown in Figure 13, Figure 14, Figure 15, and Figure 16). According to Figure 17, Figure 18, and Figure 19 the magnetic flux density is highest between the top of the coil and the aluminum disk because the field lines are confined in this small region. Subsequently, eddy currents are induced in the aluminum disk to oppose the magnetic flux. The phi-directioned eddy currents and the radial component of the magnetic field result in an upward force with a peak of 23 kN (see Figure 12). After 0.3 ms, the aluminum disk has moved 2mm and at this distance the radial component of the field has diminished considerably. Consequently, the force approaches zero although the current is still quite high.

Current distribution

Initially the current density is highest towards the top surface of the coil facing the aluminum disk due to the skin effect. Once the current reaches its peak, the current density is uniformly distributed because then there is no change in magnetic flux and no eddy currents are induced in the coil. After 0.2 ms when the current pulse starts decreasing, the surface current density becomes highest at the bottom side of the coil. This is due to that the eddy currents reverse their direction to oppose the decrease in magnetic flux (see Figure 13, Figure 14, Figure 15, Figure 16).

The eddy currents in the aluminum disk are concentrated at the surface because the field lines do not penetrate more than 3 mm. The penetration depth at different instants of time can be assessed by looking at Figure 20 that shows the magnetic flux density along a vertical line starting from point (0.038, 0.004) to point (0.038, 0.014) at different instants of time. At 0.01 ms, the penetration depth is 0.4 mm due to the fast increase of the current pulse and increases later on with decreasing slope.

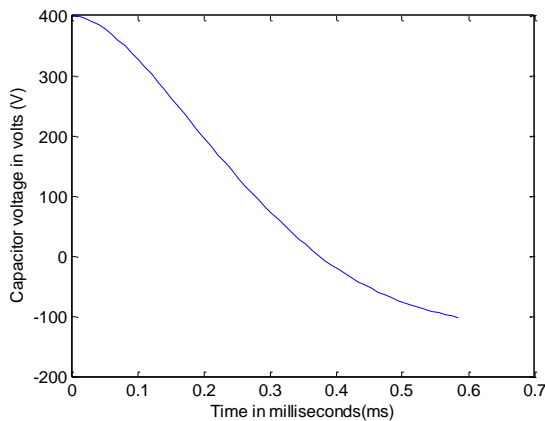


Figure 9 Capacitor voltage

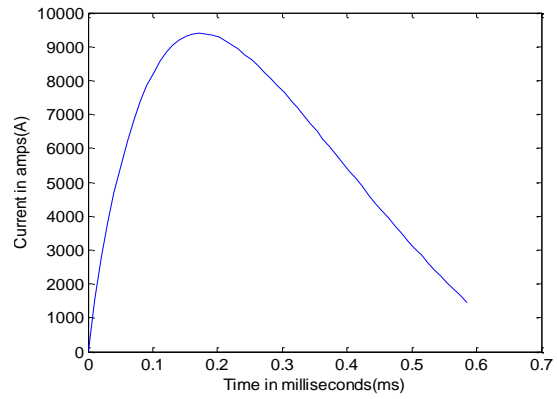


Figure 10 Current

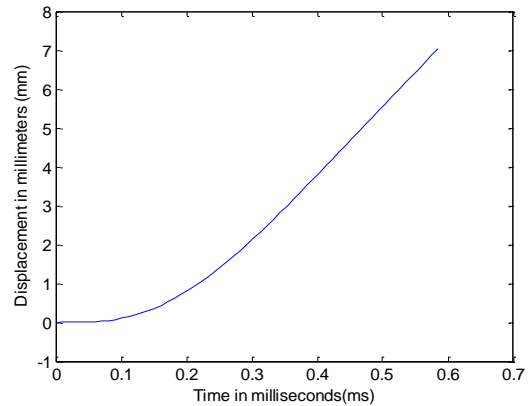


Figure 11 Aluminum disk displacement

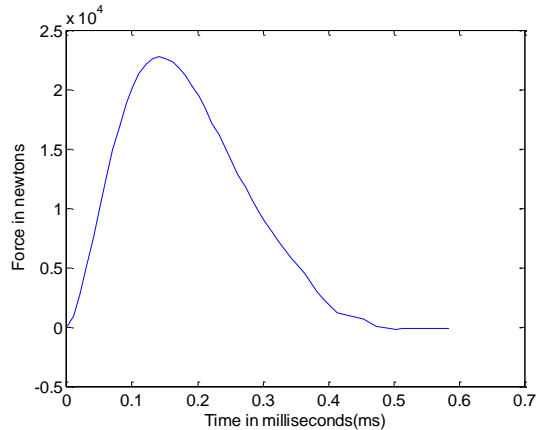


Figure 12 Exerted force on the aluminum disk vs. time

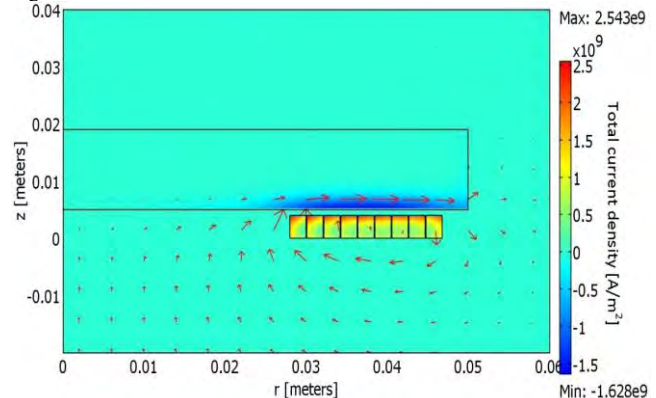


Figure 13 Time: 0.1ms, Arrow: magnetic field, Surface: Total current density

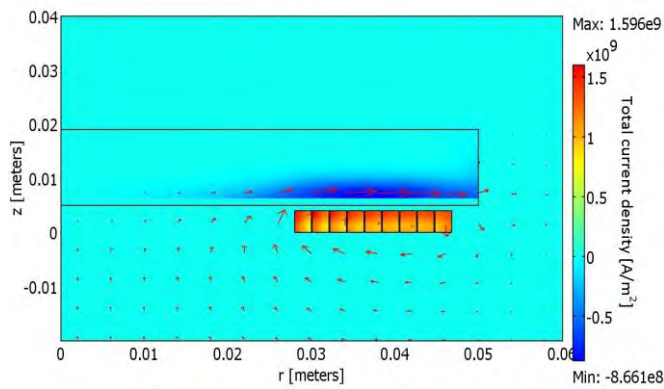


Figure 14 Time: 0.18ms, Arrow: magnetic field, Surface: Total current density

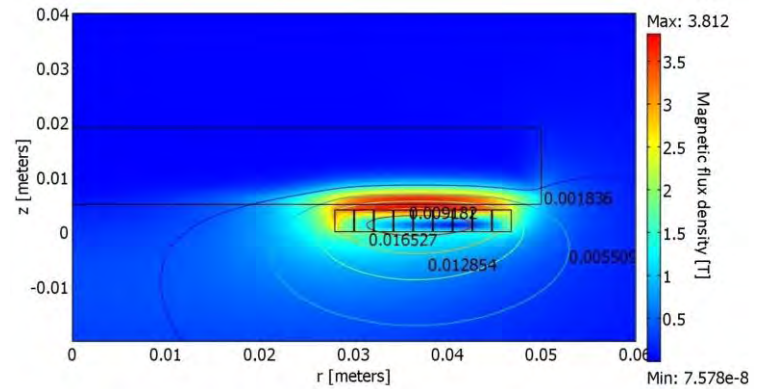


Figure 18 Time: 0.18ms, Contour lines: A [Wb/m], Surface: Magnetic flux density [T]

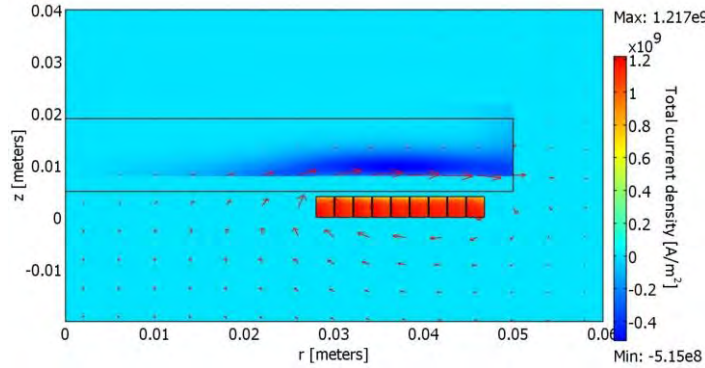


Figure 15 Time: 0.25ms, Arrow: magnetic field, Surface: Total current density

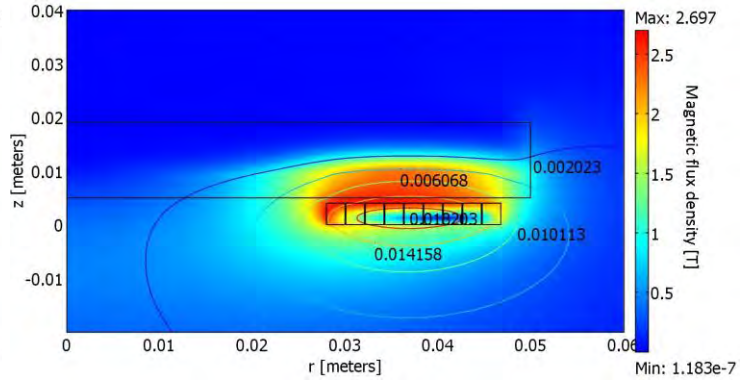


Figure 19 Time: 0.3ms, Contour lines: A [Wb/m], Surface: Magnetic flux density [T]

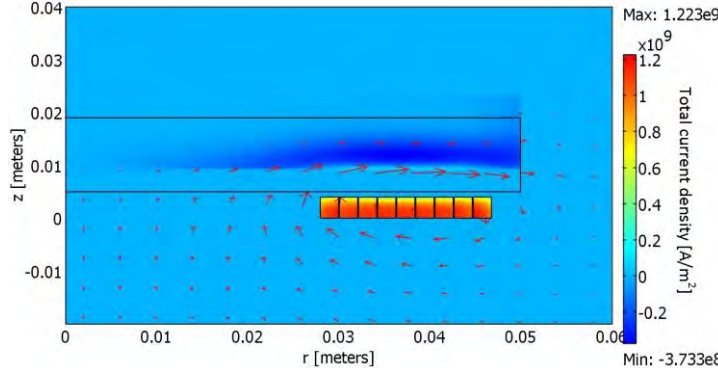


Figure 16 Time: 0.3ms, Arrow: magnetic field, Surface: Total current density

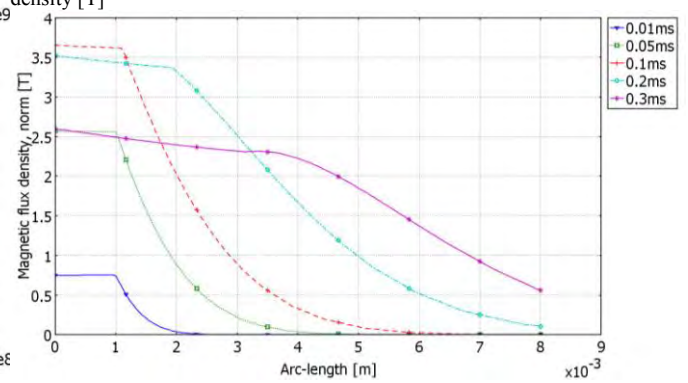


Figure 20 Magnetic flux density at different instants along the arc length

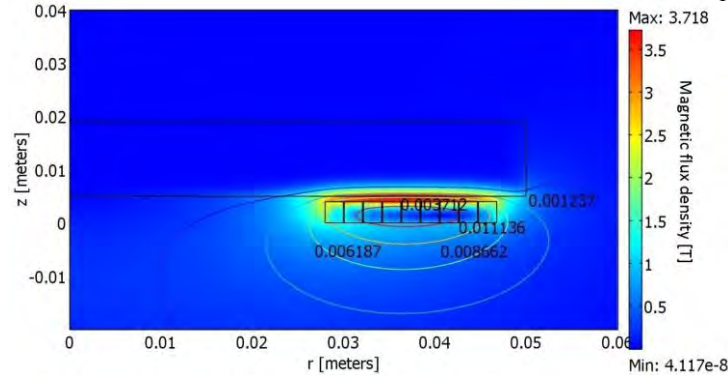


Figure 17 Time: 0.1ms, Contour lines: A [Wb/m], Surface: Magnetic flux density [T]

VI. CONCLUSIONS

The TC has many promising applications especially when there is a need for systems containing fast electromechanical actuators. This paper has shown that with the help of the presented experimentally validated Multiphysics finite element transient model, it is possible to design a TC to meet the needed requirements. Based on the drive circuit and voltage level, the imposed forces can be calculated. Consequently, the speed and distance of the moving armatures with respect to time can be determined. Moreover, this tool can be used to study several case studies to determine the sensitivity and performance of a TC with different design characteristics. Subsequently, this knowledge can shed light for future optimization procedures.

VII. REFERENCES

- [1] N. Barry. (1999). Elihu Thomson's jumping ring in a levitated closed-loop control experiment. *IEEE TRANSACTIONS ON EDUCATION*, 42(1).
- [2] W. Li, Y. Woo Jeong, H. See Yoon, C. Seop Koh. (2010). Analysis of parameters influence on the characteristics of Thomson coil type actuator of arc eliminator using adaptive segmentation equivalent circuit method. *Journal of electrical engineering and technology*, Vol.5, pp. 282-289.
- [3] D. Fleisch (2008). *A Student's guide to Maxwell's equations*. Cambridge University Press.
- [4] WG C4.204, (2009). *Mitigation techniques of power-frequency magnetic fields originated from electric power systems*. Paris: Cigré.
- [5] A. Bissal, (2010). *Master thesis for simulation and verification of Thomson actuator systems*. KTH.
- [6] J. Magnusson, O. Hammar. (2009). *Master thesis of a fast electrical commutation switch*. KTH.
- [7] Ryder, C. and Rushton, J. and Pearce, FM (1953). *A moving-coil relay applied to modern high-speed protective systems*. *Proceedings of the IEE-Part II: Power Engineering*.
- [8] Plonsey, R. and Collin, R.E (1961). *Principles and applications of electromagnetic fields*. McGraw-Hill New York.
- [9] Thompson, MT (2000). *Eddy current magnetic levitation. Models and experiments*. *IEEE potentials*.
- [10] Niwa, Y. and Funahashi, T. and Yokokura, K. and Matsuzaki, J. and Homma, M. and Kaneko, E. (2006). *Basic investigation of a high-speed vacuum circuit breaker and its vacuum arc characteristics*. *IEE Proceedings-Generation, Transmission and Distribution*.
- [11] Alferov, D. and Budovsky, A. and Evsin, D. and Ivanov, V. and Sidorov, V. and Yagnov, V. (2008). *DC vacuum circuit-breaker. Discharges and Electrical Insulation in Vacuum, 2008. ISDEIV 2008. 23rd International Symposium on*.
- [12] Pokryvailo, A. and Maron, V. and Melnik, D. (1999). *Review of opening switches for long-charge fieldable inductive storage systems. 12th IEEE International Pulsed Power Conference, 1999. Digest of Technical Papers*.
- [13] Meyer, J.M. and Rufer, A. and AG, A.B.B.S. and Turgi, S. (2006). *A DC hybrid circuit breaker with ultra-fast contact opening and integrated gate-commutated thyristors (IGCTs)*. *IEEE Transactions on Power Delivery*.
- [14] Atmadji, AMS and Sloot, JGJ. (1998). *Hybrid switching: A review of current literature. Energy Management and Power Delivery, 1998. Proceedings of EMPD'98. 1998 International Conference on*.
- [15] Meyer, J.M. and Duffour, H. and Martin, S. (2004). *Electrical coil module, an electrical coil comprising such modules, and actuation mechanism including such a coil and a circuit breaker comprising such an actuation mechanism*. *Google Patents. US Patent 6,760,202*.